FEMS Microbiology Ecology, 92, 2016, fiw048

doi: 10.1093/femsec/fiw048
Advance Access Publication Date: 2 March 2016
Research Article

RESEARCH ARTICLE

# Photochemical alteration of dissolved organic matter and the subsequent effects on bacterial carbon cycling and diversity

Christian Lønborg[1,2,*], Mar Nieto-Cid[3], Victor Hernando-Morales[4], Marta Hernández-Ruiz[4], Eva Teira[4] and Xosé Antón Álvarez-Salgado[3]

[1]Australian Institute of Marine Science, PMB 3, Townsville MC, QLD 4810, Australia, [2]Centre for Sustainable Aquatic Research, College of Science, Wallace Building, Swansea University, Swansea SA2 8PP, UK, [3]CSIC, Instituto de Investigacións Mariñas, Eduardo Cabello 6, 36208 Vigo, Spain and [4]Departamento de Ecoloxía e Bioloxía Animal, Universidade de Vigo, 36200 Vigo, Spain

*Corresponding author: Australian Institute of Marine Science, PMB 3, Townsville MC, QLD 4810, Australia. Tel: +61-7-4753-4382; Fax: +61-7-4772-5852; E-mail: clonborg@gmail.com

**One sentence summary:** Sunlight exposure impacts different organic matter sources differently, which impacts the physiology and community composition of the bacteria degrading it.

**Editor:** Gary King



## ABSTRACT

The impact of solar radiation on dissolved organic matter (DOM) derived from 3 different sources (seawater, eelgrass leaves and river water) and the effect on the bacterial carbon cycling and diversity were investigated. Seawater with DOM from the sources was first either kept in the dark or exposed to sunlight (4 days), after which a bacterial inoculum was added and incubated for 4 additional days. Sunlight exposure reduced the coloured DOM and carbon signals, which was followed by a production of inorganic nutrients. Bacterial carbon cycling was higher in the dark compared with the light treatment in seawater and river samples, while higher levels were found in the sunlight-exposed eelgrass experiment. Sunlight pre-exposure stimulated the bacterial growth efficiency in the seawater experiments, while no impact was found in the other experiments. We suggest that these responses are connected to differences in substrate composition and the production of free radicals. The bacterial community that developed in the dark and sunlight pre-treated samples differed in the seawater and river experiments. Our findings suggest that impact of sunlight exposure on the bacterial carbon transfer and diversity depends on the DOM source and on the sunlight-induced production of inorganic nutrients.

**Keywords:** dissolved organic matter; solar radiation; bacterial diversity; bacterial carbon demand; bacterial growth efficiency

## INTRODUCTION

Microbial activity in aquatic systems is mainly regulated by the energy and nutrients contained within the dissolved organic matter (DOM) pool (Hedges 2002). Coastal waters are the most productive and biogeochemically active marine ecosystems, and therefore play key roles in the production and degradation of DOM (Wollast 1998; Lønborg and Álvarez-Salgado 2012). DOM in coastal waters originates from either autochthonous or allochthonous sources; autochthonous DOM is produced within the system, primarily by macrophytes (Søndergaard 1981) and planktonic organisms (Kawasaki and Benner 2006; Lønborg *et al.* 2009), whereas allochthonous DOM is mainly of terrestrial origin (Sobczak *et al.* 2005). The combined effects of both

**Received:** 26 October 2015; **Accepted:** 28 February 2016

photochemical and microbial processes have been considered the main factor responsible for the degradation of natural DOM (Tranvik and Bertilson 2001). In addition, both processes are also able to produce recalcitrant DOM with lifetimes of years to millennia (Miller and Moran 1997; Benner and Biddanda 1998; Obernosterer, Reitner and Herndl 1999). Therefore, DOM in coastal waters is a complex mixture of exudates, leachates, and degradation and condensation products that varies widely in elemental composition and molecular structure and, consequently, in reactivity.

Given that heterotrophic bacteria are the major biological DOM sink, they regulate whether the degraded compounds are used for biomass or energy production. The ratio between bacterial production (BP) and the sum of BP and bacterial respiration (BR) has been termed the bacterial growth efficiency (BGE). This ratio varies widely (from <1 to 90%) depending on the bacterial community composition (Reinthaler, Winter and Herndl 2005), nutrient and DOM bioavailability (e.g. Rivkin and Anderson 1997; Apple and del Giorgio 2007; Lønborg *et al.* 2010a), water temperature (Rivkin and Legendre 2001) and UV-light exposure (Lønborg *et al.* 2013). The heterotrophic bacterial community consists of members from various phylogenetic lineages, with the distribution and abundance of these species being controlled by both biological and chemical factors (Fuhrman *et al.* 2006; Giovannoni and Vergin 2012). However, much less is known about how shifts in community structure may influence the microbial carbon cycling.

Photochemical reactions induced by solar radiation, especially in the UV range of the spectrum (UV-B, 280–315 nm; UV-A, 315–400 nm), are particularly important in coastal waters with high loads of coloured allochthonous DOM, where they have been shown to transform DOM into labile inorganic (mainly $NH_4^+$ and $HPO_4^{2-}$) and organic (e.g. amino acids) compounds that can support bacterial respiration and biomass production (e.g. Moran and Zepp 1997; Obernosterer and Benner 2004). In addition, photochemical processes have also been shown to enhance the cross-linking, humification and polymerization of labile biomolecules into more recalcitrant compounds (Kieber *et al.* 1997; Benner and Biddanda 1998; Obernosterer, Reitner and Herndl 1999). These sunlight-induced reactions can be seen as the abiotic counterpart of the microbial carbon pump, which suggests that the microbial utilization of organic matter is related to the release of recalcitrant compounds that accumulate in the ocean (Jiao *et al.* 2010). Solar radiation has also been found to mineralize DOM directly to inorganic carbon species ($CO_2$ or CO), free radicals and reactive oxygen species (ROS; e.g. $H_2O_2$) (e.g. Cooper *et al.* 1989; Miller and Zepp 1995). These combined photochemical reactions have been demonstrated to have a complex impact on the microbial community activity resulting in enhanced, negative, mixed or no effect (see Mopper, Kieber and Stubbins 2015 for overview). Some studies hypothesize that these variable responses to sunlight exposure are linked with the DOM origin with recently produced autochthonous DOM getting less and allochthonous DOM more bioavailable to bacteria upon irradiation, while others have found the contrary (e.g. Benner and Ziegler 2000; Sulzberger and Durisch-Kaiser 2009). While numerous studies have addressed the link between DOM photochemistry and bacterial growth, only a few (if any) investigated how changes in DOM sources and sunlight exposure influence the bacterial activity and diversity in coastal waters. Since the impact of photochemistry on DOM and bacterial activity depends on the chemical composition, changes in the exposure to sunlight and DOM source could impact the microbial community differently.

In this study, we assessed the impact of photo-alteration on DOM derived from specific aquatic sources (seawater, eelgrass and river water) and the subsequent impact of this exposure on the bacterial carbon cycling and community structure. We hypothesized that the bacterial community response will vary depending on the DOM source and sunlight exposure. This hypothesis was tested using laboratory incubations where sunlight-altered DOM was added to surface seawater from the coastal upwelling area of the Ría de Vigo (N. W. Iberian Peninsula) and changes in coloured dissolved organic matter (CDOM) optical properties and bacterial abundance, activity (production and respiration) and diversity were measured over a period of 4 days.

## MATERIALS AND METHODS

### Site description and sample treatments

In order to determine the impact of sunlight on specific DOM sources and the subsequent effects of the addition of these materials on the bacterial community of the Ría de Vigo, we collected DOM from 3 different sources: marine surface water, river water and DOM leached from leaves of the eelgrass *Zostera marina*.

Surface seawater was collected in the coastal upwelling system of the Ría de Vigo. This coastal embayment is influenced by wind-driven upwelling and downwelling episodes, with northerly winds resulting in upwelling, which prevailed during our sampling period (late spring). The seawater sample was collected on 30 May 2012 in the middle of the Ría de Vigo, a suitable site for evaluating the influence on the whole embayment (Nogueira, Pérez and Ríos 1997). The water was collected at 5 m depth using a 12-L acid-cleaned Niskin bottle and combined into a 50 L acid-washed and aged polyethylene container. After collection, the sample water was kept in the dark until processed at the base laboratory. Water temperature was measured immediately after collection, while aliquots for the analysis of salinity were collected and measured in the laboratory using an Autosal 8400A. Material for chlorophyll *a* (Chl *a*) determination was collected by filtering seawater (200 mL) through a GF/F filter and analysed after 90% acetone extraction with a Turner Designs 10000R fluorometer.

Seawater filtrations were started within 1 h after collection. One part was filtered through pre-combusted (450°C for 4 h) GF/C filters to establish a microbial culture to be used in all experiments. This was kept in the dark at 15°C until use. These were the same conditions used for the incubation study and ensured that the added microbial community was adapted to these conditions. The changes measured during our experiments in the microbial community was therefore only due to the changes in the organic matter sources and/or sunlight exposure. The other part of the seawater was gravity filtered through a dual-stage (0.8/0.2 $\mu$m) filter cartridge (Pall-Acropak Supor membrane), which had been pre-washed with Milli-Q (>10 L). The seawater was thereafter used both as the control treatment and to dilute the DOM obtained from the river water and eelgrass leaves.

In total 20 L of river water was collected in the main tributary to the Ría de Vigo, River Oitabén-Verdugo. This river is not significantly affected by industrial or sewage waste, has a drainage area of 350 $km^2$ and receives a rainfall of 2500 mm per year, which results in an average flow of 15 $m^3\ s^{-1}$ (Gago *et al.* 2005). The water samples were taken in the upstream limit of the freshwater–seawater interface. After collection the

sample water was kept in the dark until filtration commenced at the base laboratory, about 2 h later. The river water was gravity filtered through a dual-stage (0.8/0.2 $\mu$m) filter cartridge (Pall-Acropak supor Membrane) and thereafter concentrated in a proportion of 1:10 using a metal-free tangential flow ultrafiltration system, provided with a GH2540F30 membrane (GE Power & Water – Water & Process Technologies). Only the DOM material with a molecular weight >1 kDa (representing 72% of the total pool) was used in this study.

Fresh leaves of the eelgrass *Zostera marina* were collected during low tide in the San Simon bay, in the innermost part of the Ría de Vigo. Within an hour of collection, the leaves were brought back to the base laboratory and rinsed thoroughly with the 0.2 $\mu$m-filtered seawater collected in the middle of the Ría de Vigo. The eelgrass-derived DOM was thereafter extracted by adding approx. 5 g of wet leaves to a glass bottle containing 1 L of the 0.2 $\mu$m-filtered seawater. After extraction (48 h in the dark) the water was filtered first through a pre-combusted (450°C for 4 h) GF/D filter and then through a dual-stage (0.8/0.2 $\mu$m) filter cartridge (Pall-Acropak Supor membrane).

## Experimental design

The DOM derived from river water and eelgrass leaves were added to 10 L polyethylene carboys, containing 7 L of seawater, in order to reach a dissolved organic carbon (DOC) increase of about 40 $\mu$mol $L^{-1}$, while the control seawater did not receive any addition. The samples were thereafter divided into 2 experimental treatments: dark (termed 'dark') and full sunlight treatment (termed 'UV'). The dark treatments were established by placing the sample water into UVR-transparent low density polyethylene incubators (3.5 L in each) that were covered with aluminium foil and dark plastic bags, while the UV samples were distributed into UVR-transparent low density polyethylene incubators that were left uncovered. No headspace was left in either dark or UV treatments. The samples were thereafter placed in a recirculation water bath (water depth: 25 cm) in the terrace of the laboratory and exposed to 100% natural sunlight for 4 days encompassing the natural light–dark cycle. During the sunlight exposure the incubators were almost completely covered in water (around 85%). The temperature was not specifically controlled during the exposure period but a constant flow (approx. 3 L $min^{-1}$) of cold tap water cooled the samples. This ensured that the temperature was kept constantly low, suggesting that changing temperature did not impact our UV exposure results. Incident irradiance during the UV treatments was taken from the meteorological observatory on the terrace of the base laboratory, showing that over the 4 days the UV samples were exposed to 20 MJ $m^{-2}$ $d^{-1}$ of total solar radiation. Before and after sunlight exposure, subsamples were collected for the analysis of DOC, dissolved inorganic nitrogen (DIN: $NH_4^+$, $NO_2^-$, $NO_3^-$), dissolved inorganic phosphorus (DIP: $HPO_4^{2-}$) and DOM optical properties (absorption and induced fluorescence). After the 4 days of sunlight exposure the water samples were within 15 min combined into different (dark and UV) carboys and the seawater microbial community was added in a ratio of 1 part of microbial culture, established from seawater collected in the Ría de Vigo on 30 May 2012, to 9 parts of exposed water. The water was thereafter transferred into fifteen 500 mL glass bottles per treatment (90 bottles in total) and incubated in the dark at a constant temperature of 15°C, with 3 replicate bottles being used for sub-sampling at incubation times 0, 1, 2, 3 and 4 days. The processing of the samples at initial time point started approximately 1 h after completion of the sunlight exposure. Unfiltered water from these bottles was used to follow changes in bacterial abundance (BA), diversity (using automated rRNA intergenic spacer analysis (ARISA)), bacterial production (BP) and bacterial respiration (BR). Samples for the analysis of DOC, DIN, DIP and CDOM absorption and fluorescence were collected after filtration through 0.2 $\mu$m filters (Pall Supor membrane Disc), which were placed in an acid-cleaned all-glass filtration system under low $N_2$ flow pressure. All glassware used was acid washed in 10% HCl and rinsed with Milli-Q and sample water prior to use.

## Sample analysis

Samples for BA were fixed with 25% glutaraldehyde (0.5% final concentration) for 30 min at 4°C, flash-frozen in liquid nitrogen and stored at –80°C until analysed. Thawed samples were diluted up to 10-fold in autoclaved 0.2 $\mu$m filtered TE buffer (10:1 Tris–EDTA, pH 8.0) and stained with the nucleic acid-specific dye SYBR Green I (Invitrogen/Molecular Probes) for 15 min in the dark and analysed using a FACSCalibur flow cytometer. Bacterial biomass (BB) was calculated from BA, using a carbon conversion factor of 12 fg C $cell^{-1}$, which is representative for coastal bacterial assemblages (Fukuda *et al.* 1998).

BP was measured by [$^3$H]thymidine incorporation (Fuhrman and Azam 1980). Three replicate 9.9-mL samples and 2 trichloroacetic acid killed samples were added to an aqueous stock solution of [$^3$H-methyl]thymidine (20 nmol final concentration). The samples were incubated in the dark at 15°C for 1 h, 10 mL of ice-cold trichloroacetate (TCA) was thereafter added and samples were filtered onto 0.2 $\mu$m polycarbonate filters (presoaked in non-labelled thymidine) and washed with 95% ethanol and autoclaved Milli-Q water. The filters were thereafter dried at room temperature (24 h) and mixed with 10 mL of scintillation fluid (Sigma-Fluor). The radioactivity incorporated into cells was counted using a Wallac scintillation counter. The disintegrations per minute (DPM) of the TCA-killed blank were subtracted from the DPMs of the samples. Thymidine incorporated into bacterial biomass was converted to carbon production using the theoretical conversion factors, $2 \times 10^{18}$ cells $mol^{-1}$ thymidine (Fuhrman and Azam 1980) and using the same cell-to-carbon conversion factor as for BA.

The bacterial respiration (BR) was estimated using the reduction of 2-(4-iodophenyl)-3-(4-nitro-phenyl)-5-phenyl tetrazolium chloride (INT) following Martínez-García *et al.* (2009). In brief, the activity was measured using 1 h incubations of 3 replicate samples (10 mL) and 1 formaldehyde-killed control. The incubations were terminated by adding formaldehyde and filtering onto 0.2 $\mu$m polycarbonate filters. The filters were thereafter stored frozen (–20°C) until further processing. The respiration rates derived from INT reduction (BR, in $\mu$mol $O_2$ $L^{-1}$ $h^{-1}$) were obtained by multiplying the *in vivo* INT reduction rate (in $\mu$mol INTF $L^{-1}$ $h^{-1}$) by an empirically derived conversion factor of 12.8.

The instantaneous bacterial carbon demand (BCD) was calculated as the sum of C-converted BP and BR:

$$BCD = BP + BR \quad (1)$$

The instantaneous bacterial growth efficiency (BGE) was calculated as BP divided by the sum of BP and BR:

$$BGE = BP/(BP + BR) \quad (2)$$

The integrated BCD ($BCD_{int}$) over the incubation period was calculated as the bioavailable DOC (BDOC):

$$BCD_{int} = BDOC \quad (3)$$

The integrated BGE over the 4 days ($BGE_{int}$) was calculated as the net growth in bacterial biomass between day 0 and maximum abundance (BG; $BG = BB_{max} - BB_{min}$) divided by BDOC:

$$BGE_{int} = BG/BDOC \quad (4)$$

The DOC samples were collected into pre-combusted (450°C, 12 h) glass ampoules and preserved with 50 $\mu$L 25% $H_2PO_4$ to 10 mL sample. DOC was measured using a Shimadzu TOC analyser (Pt catalyst) and 3 to 5 replicate injections of 150 $\mu$L were performed per sample. Concentrations were determined by subtracting a Milli-Q blank and dividing by the slope of a daily standard curve of potassium hydrogen phthalate. Using the deep ocean reference provided by Prof. D. A. Hansell, University of Miami (Sargasso Sea deep water 2600 m) we obtained a concentration of 46.0 ± 2.0 $\mu$mol $L^{-1}$ (mean ± SD), with the DOC value provided by the reference laboratory being 44.0 ± 1.5 $\mu$mol $L^{-1}$. The difference between the initial ($DOC_0$) and minimum DOC ($DOC_{min}$) concentration over the 4 days' incubation was here defined as the bioavailable DOC (BDOC).

DIN and DIP samples were collected into 50 mL acid-washed polyethylene bottles and measured using standard segmented flow analysis (SFA) as described in Hansen and Koroleff (1999).

Absorption spectra (250–600 nm) of CDOM were measured on a Beckman Coulter DU 800 spectrophotometer using Milli-Q water as a blank. Before analysis samples were warmed to room temperature and absorbance was measured with 1 nm increments using a 10 cm quartz cuvette. The absorption coefficient at any wavelength, $a_{CDOM}(\lambda)$ ($m^{-1}$), was calculated as:

$$a_{CDOM}(\lambda) = 2.303 \cdot [Abs(\lambda) - Abs(600-750)]/0.1 \quad (5)$$

Where Abs(λ) is the absorbance at wavelength λ; Abs(600–750) is the average absorbance between 600 and 750 nm, which corrects for the residual scattering by fine size particle fractions, micro-air bubbles or colloidal material present in the sample, or refractive index differences between the sample and the reference ($m^{-1}$); the factor 2.303 converts from decadic to natural logarithms; and the denominator (0.1) is the cell path-length in metres. The estimated detection limit of this spectrophotometer is 0.001 absorbance units or 0.02 $m^{-1}$. As the treatments had different DOC concentrations, we standardize the CDOM absorption by calculating the C-specific absorption coefficient CDOM absorption spectra ($a^*_{CDOM}(\lambda)$). The C-specific absorption coefficient at 254 nm, known as SUVA (Weishaar *et al.* 2003), was calculated by dividing the decadic $a_{CDOM}(254)$ by the DOC concentration and expressed in litres per milligram per metre.

The CDOM spectral slope (S) of the C-specific absorption spectra was modelled as:

$$a^*_{CDOM}(\lambda) = a^*_{CDOM}(375) \cdot e^{-S \cdot (\lambda - 375)} \quad (6)$$

where $a^*_{CDOM}(\lambda)$ is the carbon-specific absorption coefficient at wavelength λ, $a^*_{CDOM}(375)$ is the C-specific absorption coefficient at the reference wavelength of 375 nm, and S is the spectral slope coefficient of the absorption curve calculated over the range 250–600 nm. The CDOM spectral slopes were also calculated over two narrow wavelength ranges, S(275–295) and S(350–400), using linear regressions of the natural log-transformed $a_{CDOM}(\lambda)$ spectra. These slopes were used to calculate the CDOM spectral slope (S(275–295)/S(350–400)) ratio ($S_R$) (Helms *et al.* 2008).CDOM fluorescence emission excitation matrices (EEMs) and single-point measurements were performed on a Perkin Elmer LS 55 luminescence spectrophotometer equipped with a xenon discharge lamp, equivalent to 20 kW for 8 $\mu$s duration. Measurements were performed at a constant temperature of 20°C in a 1 cm quartz fluorescence cell. The EEMs were generated by combining 22 fluorescence emission spectra from 300 to 560 nm at excitation wavelengths ranging from 240 to 450 nm at 10 nm intervals. Point excitation/emission (Ex/Em) measurements were performed at wavelengths characteristic of peak-A (general humic-like substances, average Ex/Em, 250 nm/435 nm), peak-C (terrestrial humic-like substances, at Ex/Em wavelengths of 340 nm/440 nm), peak-M (marine humic-like substances, average Ex/Em, 320 nm/410 nm) and peak-T (protein-like substances, average Ex/Em, 280 nm/320 nm) (Coble 1996; Lønborg *et al.* 2010b). The fluorescence measurements were normalized to the Raman area using daily spectra of Milli-Q water (Lawaetz and Stedmon, 2009). As the treatments had different DOC concentrations, we standardize the FDOM values by calculating the carbon-specific FDOM as the FDOM signal divided by the DOC concentration. The limit of detection, calculated as 3 × the standard deviation of the blank, was 0.03 QSU for peak-A, 0.05 QSU for peak-C and 0.02 QSU for peak-M and peak-T.

## Automated rRNA intergenic spacer analysis

Automated rRNA intergenic spacer analysis (ARISA) was conducted with DNA from the initial community and at the end of each experiment, for characterizing the initial and final microbial community for each treatment. For the initial community, samples were prefiltered through a 1.2 $\mu$m pore-size filter (Kleenpak Capsule HDCII), and subsequently 2 L was filtered on a 0.2 $\mu$m pore-size polycarbonate filter (Nuclepore Whatmann, 47 mm filter diameter). At the end of the experiments 0.5–1 L from each treatment was filtered on a 0.2 $\mu$m pore-size polycarbonate filter (Nuclepore Whatmann, 47 mm filter diameter). Filters were then stored at –80°C until DNA extraction. Microbial community DNA was extracted using Ultra Clean Soil DNA isolation kit (MoBio Laboratories, Inc.) and quantified in a Nanodrop. Bacterial ARISA was performed using ITSF/ITSReub primer set (Thermo Scientific) previously described by Cardinale *et al.* (2004). The PCR reaction (25 $\mu$L) contained final concentrations of 1x PCR buffer (Genecraft), 2.5 mmol $L^{-1}$ $MgCl_2$ (Genecraft), 250 $\mu$mol $L^{-1}$ of each dNTP (Genecraft), 250 nmol $L^{-1}$ of universal primer ITSF (5′-GTCGTAACAAGGTAGCCGTA-3′) and eubacterial ITSReub (5′-GCCAAGGCATCCACC-3′) (Cardinale *et al.* 2004), the former being labelled at the 5′ end with the fluorescein amidite dye (6-FAM), 40 ng $\mu L^{-1}$ bovine serum albumin, 3.5 U of BioThermD-™ Taq DNA Polymerase (GeneCraft) and approx. 0.13 ng $\mu L^{-1}$ of template DNA. The reaction mixture was held at 94°C for 2 min followed by 32 cycles of amplification at 94°C for 15 s, 55°C for 30 s and 72°C for 3 min, with a final extension of 72°C for 10 min. PCR samples were conducted by duplicates for each DNA extraction (this compensates for any anomalously running fragments both in the samples and in the standards). Amplification products were migrated by capillary electrophoresis on a 50 cm capillary ABI Prism 3730XL DNA analyser (Applied Biosystems) at Genoscreen (www.genoscreen.fr/). The standardized migration cocktail contained 0.5 $\mu$L of amplification product, 0.25 $\mu$L of internal size standard LIZ 1200 (20–1200 pb, Applied Biosystems) and 8.75 $\mu$L of deionized Hi-Di formamide (Applied Biosystems). The mixture was denatured for 5 min at 95°C and kept on ice before being further processed by the sequencer.

Capillary electrophoresis parameters were as follows: 10 kV (run voltage), 1.6 kV (injection voltage), 22 s (injection time) and 63°C (oven temperature). Resulting electropherograms were analysed using DAx software (Data Acquisition and Analysis Software, Van Mierlo Software). Internal size standards were built by using a second-order least-squares method and local Southern method. Profiles were double checked manually for perfect internal size standard fit and stable baselines. Baselines were then extracted, and subsequently, peak sizes, heights and absolute areas were determined. The same process was done for the PCR negative sample. From the negative sample, the 95th percentile was calculated for the height measurement, and used as a threshold. Sample with peak heights below the 95th percentile were discarded (the 95th percentile of each duplicated PCR negative presented values of 9 and 8.7 relative fluorescence intensity (RFI) respectively).

Profile peaks were binned and rearranged by operational taxonomic units (OTUs) by using R automatic binning and interactive binning scripts (Ramette 2009). Binning was carried out independently of the sample (peaks from all samples together). Only peaks in the range 200 to 1200 bp and with values above 0.09% of total RFI were taken into account. Peaks from duplicates were manually checked using binned-OTU tables, to avoid erroneous OTU divisions due to rearrangement of all samples together.

### Statistical analyses

In this paper *t*-tests were performed to test the significance of the differences observed in bacterial abundance and activity between dark and UV-irradiation incubations (Sokal and Rohlf 1995). The confidence level was set at 95%, with all statistical analyses conducted in Statistica 6.0. Differences in ARISA fingerpints between initial and final community as well as among treatments were analysed by comparing Bray–Curtis similarities using the package Primer 6 and Permanova+. A log $X + 1$ transformation of ARISA relative abundance was used to reduce the dominant contribution by a small number of highly abundant species to the Bray–Curtis analysis (despite results being very similar with and without transformations). Similarity patterns among samples were then examined using a hierarchical cluster analysis. Dendograms were generated using the group average method, and a similarity profile (SIMPROF) test (999 permutations) was applied to test for significantly similar clusters.

## RESULTS

### Effects of sunlight on inorganic nutrients and dissolved organic matter

The recorded surface seawater salinity (35.4), temperature (17.4°C), Chl *a* (4.3 mg $m^{-3}$) and nutrient levels ($HPO_4^{2-}$: 0.04 ± 0.03 $\mu$mol $L^{-1}$; $NO_3^-$+$NO_2^-$: 0.14 ± 0.02 $\mu$mol $L^{-1}$; $NH_4^+$: 1.21 ± 0.17 $\mu$mol $L^{-1}$) were similar to typical late spring conditions in the Ría de Vigo (Nogueira, Pérez and Ríos 1997). In all incubations, exposure to sunlight resulted in increased $NH_4^+$ concentrations relative to the dark control, while increased $HPO_4^{2-}$ concentrations were found in the seawater and eelgrass experiments (Table 1). The DOC concentrations before irradiation were 99 ± 1 $\mu$mol $L^{-1}$ in the seawater, 131 ± 4 $\mu$mol $L^{-1}$ in the eelgrass and 154 ± 2 $\mu$mol $L^{-1}$ in the river samples (Table 1). The light treatment caused a 5 ± 2% decrease in DOC concentrations in the seawater experiments, while 12 ± 8% and 9 ± 3% lower concentrations were found in the eelgrass and river samples, respectively (Table 1). The UV exposure resulted in a lower concentration of bioavailable DOC (BDOC) over the 4 days' incubation compared with the dark treatment in the seawater (8 ± 1 vs 17 ± 4 $\mu$mol $L^{-1}$) and river experiments (19 ± 1 vs 26 ± 1 $\mu$mol $L^{-1}$), while increased BDOC levels were found in the eelgrass experiment (38 ± 2 vs 20 ± 5 $\mu$mol $L^{-1}$) (Table 1).

The initial C-normalized CDOM absorption spectra measured from 250 to 600 nm showed that the river DOM was more coloured than the seawater and eelgrass treatments (Fig. 1a–c). The maximum photoproduction of CDOM was found at wavelengths below 260 nm in both the seawater and eelgrass experiments, while the largest loss of carbon-specific absorption for all analysed wavelengths and treatments was found around 310 nm in the river experiments (Fig. 1d). The C-normalized spectral slope determined by fitting the absorption spectra to a single exponential decay function (Eq. 6) showed significantly higher slopes in the sunlight-exposed eelgrass and river experiments (*t*-test, $P < 0.05$). The C-normalized absorption at 254 nm (SUVA) was here taken as a measure of the aromaticity and abundance of carbon double bonds in the DOM (Weishaar *et al.* 2003) present in the dark and sunlight-exposed samples. Sunlight exposure did not significantly impact the SUVA in any of the experiments. The spectral slope ratio ($S_R$), which is inversely correlated to the molecular weight, increased in all UV light-exposed samples (Table 1), suggesting a photochemically induced decrease in the average molecular weight (Helms *et al.* 2008).

There were clear differences in the C-specific FDOM signals between treatments both before and after 4 days' sunlight exposure especially in the river experiment, suggesting differences in the CDOM chemical composition (Fig. 2 and Table 1). The initial seawater experiments had the generally lowest FDOM signals, eelgrass had intermediate and river samples the highest values (Fig. 2 and Table 1). For the case of the protein-like fluorescence, the eelgrass showed the highest C-specific fluorescence, while the river samples had a generally higher humic contribution (Fig. 2 and Table 1). The C-normalized fluorescence signals of the humic- and protein-like substances decreased in all sunlight-exposed samples showing the largest impact on the humic substances in the river experiment (Fig. 2 and Table 1).

### Bacterial response to DOM of different origin and the effect of solar radiation

Initial bacterial abundances (BA) were the same (~2 × $10^5$ cells $mL^{-1}$) in all treatments (Fig. 3). Bacterial abundances increased in all experiments (Fig. 3) following the consumption of DOC (Table 1), reaching maximum abundances of 23 × $10^5$ (dark) and 27 × $10^5$ cells $mL^{-1}$ (UV) in the seawater, 24 × $10^5$ (dark) and 35 × $10^5$ cells $mL^{-1}$ (UV) in the eelgrass, and 17 × $10^5$ (UV) and 19 × $10^5$ cells $mL^{-1}$ (dark) in the river incubations (Fig. 3). These increases in BA corresponded to an average bacterial biomass growth (BG) of 2.07 ± 0.05 (dark) and 2.44 ± 0.03 $\mu$mol $L^{-1}$ (UV) in the seawater, 2.22 ± 0.04 (dark) and 3.27 ± 0.04 $\mu$mol $L^{-1}$ (UV) in the eelgrass and 1.45 ± 0.04 (dark) and 1.72 ± 0.04 $\mu$mol $L^{-1}$ (UV) in the river experiments (Table 2). The BA was not significantly different in the dark and UV treatments in the 3 experiments. The initial BP varied between 0.14 ± 0.09 (river–UV) and 1.47 ± 0.02 $\mu$mol $L^{-1}$ (seawater–UV), with higher initial levels in UV-exposed seawater and eelgrass samples, whereas higher levels were found in the dark samples in the river incubations (Fig. 3 and Table 2). The integrated BP was larger in the UV seawater (2.47 ± 0.55 (dark) vs 2.89 ± 0.31 $\mu$mol $L^{-1}$ (UV)) and eelgrass incubations (1.61 ± 0.24 (dark) vs 3.25 ± 0.55 $\mu$mol $L^{-1}$ (UV)), while lower levels were found in the river experiments (2.18 ± 0.42 (dark) vs 1.29 ± 0.25

**Table 1.** Concentrations of phosphate ($HPO_4^{2-}$), nitrate ($NO_3^-$), nitrite ($NO_2^-$) and ammonium ($NH_4^+$), the C-specific CDOM absorption coefficient at 254 nm (SUVA) and spectral slope in the 250–600 nm wavelength range (S), ratio of CDOM spectral slopes (S(275–295)/S(350–400) ratio ($S_R$)), C-specific general (peak-A*), terrestrial (peak-C*) and marine humic-like substances (peak-M*) and protein-like substances (peak-T*), initial concentrations of dissolved organic carbon (DOC) before and after 4 days in darkness (dark) or exposed to natural sunlight (UV). The DOC concentration at incubation day 0 ($DOC_0$) and the minimum concentration ($DOC_{Min}$) are also shown together with the bioavailable fraction (BDOC) before and after UV-light exposure. Values are means ± standard deviation; —, not measured.

| | Seawater | | | Eelgrass | | | River | | |
|---|---|---|---|---|---|---|---|---|---|
| | Before UV | Dark | UV | Before UV | Dark | UV | Before UV | Dark | UV |
| $HPO_4^{2-}$ ($\mu$mol $L^{-1}$) | 0.06 ± 0.02 | 0.18 ± 0.08 | 0.37 ± 0.11 | 0.21 ± 0.08 | 0.21 ± 0.12 | 0.30 ± 0.08 | 0.25 ± 0.01 | 0.25 ± 0.05 | 0.24 ± 0.20 |
| $NO_3^-$ ($\mu$mol $L^{-1}$) | 0.09 ± 0.01 | 0.08 ± 0.02 | 0.30 ± 0.01 | 0.08 ± 0.02 | 0.10 ± 0.02 | 0.09 ± 0.02 | 0.07 ± 0.08 | 0.09 ± 0.01 | 0.13 ± 0.01 |
| $NO_2^-$ ($\mu$mol $L^{-1}$) | 0.06 ± 0.01 | 0.13 ± 0.10 | 0.22 ± 0.02 | 0.08 ± 0.01 | 0.14 ± 0.01 | 0.11 ± 0.01 | 0.09 ± 0.02 | 0.11 ± 0.01 | 0.14 ± 0.01 |
| $NH_4^+$ ($\mu$mol $L^{-1}$) | 1.60 ± 0.17 | 1.28 ± 0.26 | 2.17 ± 0.33 | 0.62 ± 0.06 | 0.46 ± 0.30 | 2.61 ± 0.76 | 1.63 ± 0.34 | 1.12 ± 0.35 | 2.31 ± 0.31 |
| SUVA (L $mg^{-1}$ $m^{-1}$) | 0.95 ± 0.04 | 0.96 ± 0.04 | 1.03 ± 0.03 | 1.16 ± 0.03 | 1.17 ± 0.04 | 1.38 ± 0.04 | 1.99 ± 0.06 | 1.99 ± 0.06 | 1.92 ± 0.06 |
| S ($nm^{-1}$) | 0.0171 ± 0.0001 | 0.0171 ± 0.0001 | 0.0167 ± 0.0001 | 0.0092 ± 0.0001 | 0.0092 ± 0.0001 | 0.0110 ± 0.0001 | 0.0125 ± 0.0001 | 0.0124 ± 0.0001 | 0.0156 ± 0.0001 |
| $S_R$ | 1.59 ± 0.04 | 1.59 ± 0.05 | 1.98 ± 0.05 | 1.38 ± 0.04 | 1.38 ± 0.06 | 1.74 ± 0.12 | 0.84 ± 0.01 | 0.84 ± 0.02 | 1.34 ± 0.03 |
| Peak-A* ($\times 10^8$ L $mg^{-1}$ $m^{-1}$) | 4.02 ± 0.09 | 4.97 ± 0.15 | 4.13 ± 0.09 | 3.66 ± 0.07 | 3.77 ± 0.08 | 3.81 ± 0.06 | 10.90 ± 0.03 | 12.00 ± 0.07 | 6.38 ± 0.09 |
| Peak-C* ($\times 10^8$ L $mg^{-1}$ $m^{-1}$) | 1.66± 0.05 | 1.81 ± 0.01 | 1.50 ± 0.06 | 2.06 ± 0.07 | 1.92 ± 0.03 | 1.68 ± 0.04 | 5.50 ± 0.08 | 5.75 ± 0.03 | 2.50 ± 0.04 |
| Peak-M* ($\times 10^8$ L $mg^{-1}$ $m^{-1}$) | 1.75 ± 0.11 | 1.82 ± 0.03 | 1.52 ± 0.03 | 1.93 ± 0.01 | 1.62 ± 0.03 | 1.50 ± 0.06 | 4.33 ± 0.08 | 4.48 ± 0.02 | 2.39 ± 0.04 |
| Peak-T* ($\times 10^8$ L $mg^{-1}$ $m^{-1}$) | 2.36 ± 0.24 | 3.17 ± 0.10 | 2.66 ± 0.08 | 3.49 ± 0.03 | 3.16 ± 0.06 | 3.44 ± 0.18 | 1.78 ± 0.01 | 2.78 ± 0.12 | 2.19 ± 0.05 |
| DOC ($\mu$mol $L^{-1}$) | 99 ± 1 | 98 ± 2 | 94 ± 2 | 131 ± 4 | 130 ± 1 | 115 ± 1 | 154 ± 2 | 149 ± 1 | 140 ± 1 |
| $DOC_0$ ($\mu$mol $L^{-1}$) | — | 96 ± 1 | 93 ± 1 | — | 117 ± 2 | 111 ± 1 | — | 140 ± 1 | 139 ± 1 |
| $DOC_{Min}$ ($\mu$mol $L^{-1}$) | — | 80 ± 1 | 85 ± 1 | — | 83 ± 3 | 73 ± 2 | — | 115 ± 1 | 121 ± 1 |
| BDOC ($\mu$mol $L^{-1}$) | — | 17 ± 4 | 8 ± 1 | — | 20 ± 5 | 38 ± 2 | — | 26 ± 1 | 19 ± 1 |

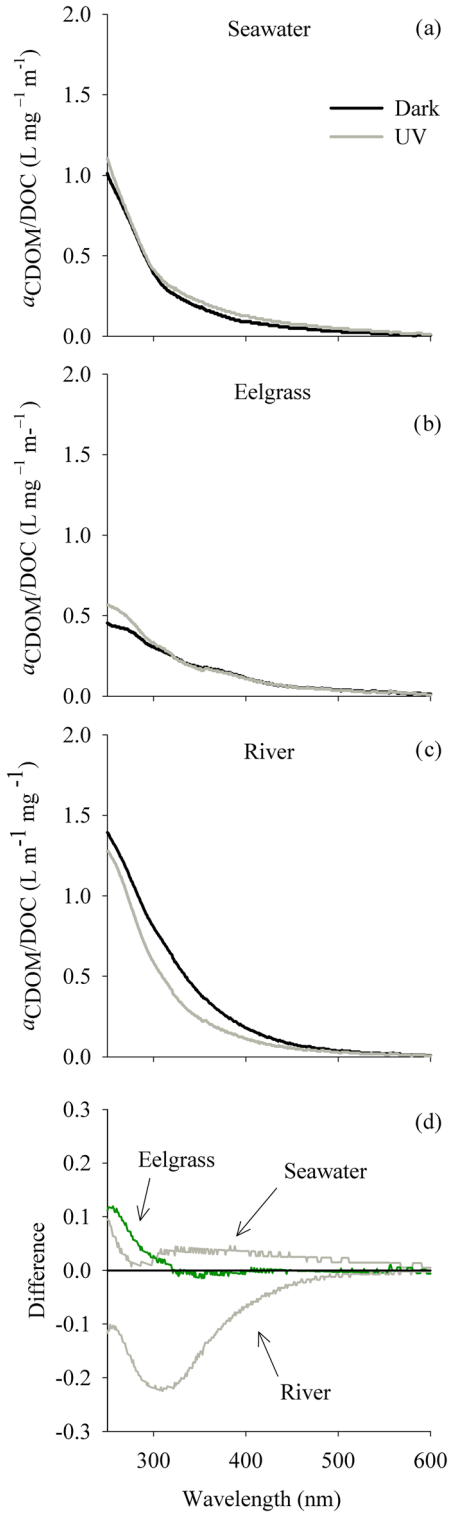


**Figure 1.** The carbon-specific absorption spectra of coloured dissolved organic matter (CDOM) after 4 days in the dark (dark) or exposed to natural sunlight (UV) in the (**a**) seawater, (**b**) eelgrass and (**c**) river experiments. The difference (dark minus sunlight samples) in the carbon-specific absorption spectra of CDOM in the seawater, eelgrass and river experiments are shown in (**d**). Note that in the case of the eelgrass and river samples, the blank subtracted was the seawater used to dilute the extracts.

$\mu$mol $L^{-1}$ (UV)) (Table 2). The BP was significantly higher in the UV treatment in the eelgrass and in the dark for the river experiments (*t*-test, $P < 0.05$, n = 4), while no significant difference was found in the seawater experiment. The instantaneous specific growth rate ($\mu$), calculated as the ratio between BP and BB (BP/BB), showed that the UV pre-exposure had contrasting effects on the initial $\mu$, with an increase in the seawater (3.90 ± 0.01 (dark) vs 5.41 ± 0.35 $d^{-1}$ (UV)) and eelgrass experiments (1.96 ± 0.70 (dark) vs 3.46 ± 1.26 $d^{-1}$ (UV)) and a decrease in the river incubations (3.50 ± 1.40 (dark) vs 0.65 ± 0.47 $d^{-1}$ (UV)) (Table 2). The $\mu$ decreased over the incubation period in all experiments reaching levels between 0.40 ± 0.09 (eelgrass–dark) and 0.88 ± 0.16 $d^{-1}$ (river–dark) at day 4 (Table 2).

The initial BR was higher in the dark treatments in all incubations (Fig. 3 and Table 2). In the seawater experiments, the BR increased after day 0 reaching maximum levels of 6.52 ± 0.41 $\mu$mol $L^{-1}$ $d^{-1}$ in the dark and 3.49 ± 0.15 $\mu$mol $L^{-1}$ $d^{-1}$ in the UV experiments (Fig. 3 and Table 2). In the eelgrass UV incubations a dramatic increase was seen after the initial day, reaching a maximum value of 19.50 ± 2.25 $\mu$mol $L^{-1}$ $d^{-1}$, while more stable levels were found in the dark incubations with a maximum of 5.39 ± 0.18 $\mu$mol $L^{-1}$ $d^{-1}$ (Fig. 3 and Table 2). In the river dark treatment the BR remained at a constant higher level (max. 8.95 ± 0.50 $\mu$mol $L^{-1}$ $d^{-1}$) than the UV pre-treated samples (max. 7.86 ± 0.61 $\mu$mol $L^{-1}$ $d^{-1}$) until incubation day 3, whereafter equal BR were found in both experiments (Fig. 3 and Table 2). The BR and integrated BR were significantly higher in the dark treatment in the seawater and river experiments, and significantly higher in the UV treated samples in the eelgrass experiment (*t*-test, $P < 0.05$, $n = 4$). In all experiments the initial cell-specific BR was lower in the UV pre-treated samples (Fig. 3j–l and Table 2). After the initial day in the seawater and river incubations the cell-specific BR was generally higher in the dark compared with the UV treatments, while a higher activity was found in the UV exposed samples in the eelgrass experiments (Fig. 3j–l and Table 2).

The initial BCD was higher in the dark compared with the UV treatments in all experiments (Fig. 4a–c and Table 2). Thereafter a continued higher BCD was found in the dark samples in the seawater and river experiments, while in the eelgrass experiment higher levels were found in the UV pre-treated samples (Fig. 4a–c and Table 2). Overall the average BCD was significantly higher in the dark samples in the seawater and river experiments, while a significantly higher BCD was found in the UV pre-exposed samples in the eelgrass experiments (*t*-test, $P < 0.04$, $n = 4$). The UV pre-treatment also decreased the integrated BCD in the seawater (23.7 ± 1.7 (dark) vs 11.7 ± 1.1 $\mu$mol $L^{-1}$ $d^{-1}$ (UV)) and river (32.3 ± 3.4 (dark) vs 23.5 ± 1.9 $\mu$mol $L^{-1}$ $d^{-1}$ (UV)) experiments, while an increase was found in the eelgrass (16.4 ± 1.0 (dark) vs 62.8 ± 10.7 $\mu$mol $L^{-1}$ $d^{-1}$ (UV)) experiment (Table 2).

The instantaneous BGE varied initially between 3 ± 1 (river–UV) and 58 ± 7% (seawater–UV) decreasing thereafter to values between 4 ± 1 (eelgrass–dark) and 14 ± 1% (seawater–UV) at incubation day 4 (Fig. 4d–f and Table 2). The initial BGE was significantly higher (*t*-test, $P < 0.01$) in the UV pre-exposed seawater experiments, while equal levels for both treatments were found in the eelgrass and river incubations (Fig. 4d–f and Table 2). The integrated BGE ($BGE_{int}$) showed highest values in the UV–seawater samples (25 ± 6%) and lowest in the dark–river samples (5 ± 1%), with no significant differences between the dark and UV pre-treatments in any of the experiments (Table 2). The instantaneous BGE averaged over the 4 days' incubation showed similar levels as the $BGE_{int}$ (Table 2).

The bacterial community composition at time zero and at the end of each experiment was compared based on ARISA

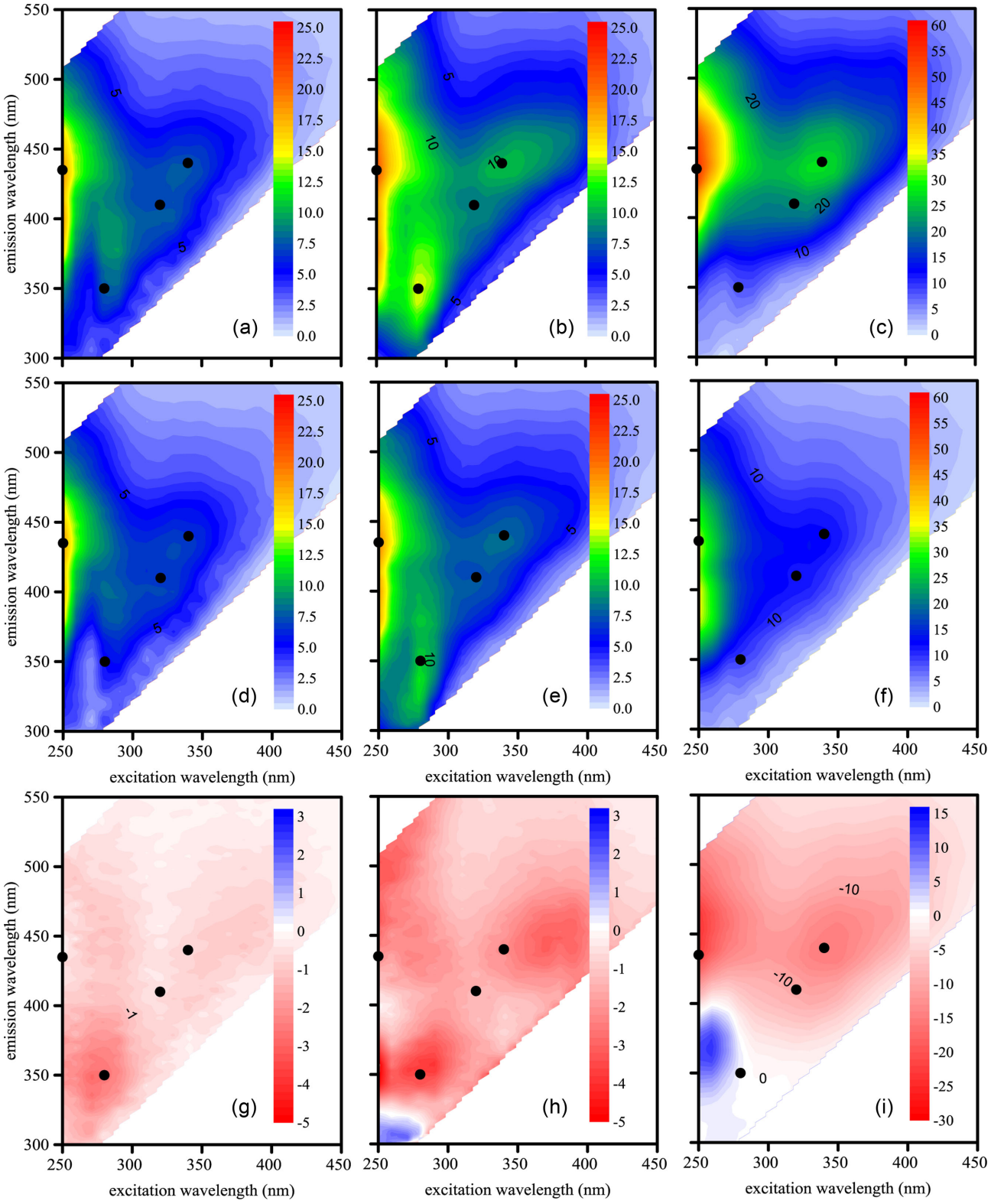


Figure 2. C-specific fluorescence excitation emission matrix of (a) seawater dark, (b) seawater UV, (c) eelgrass dark, (d) eelgrass UV, (e) river dark, (f) river UV, (g) seawater dark minus UV, (h) eelgrass dark minus UV and (i) river dark minus UV samples. Fluorescence units are $10^6$ L mg$^{-1}$ m$^{-1}$.

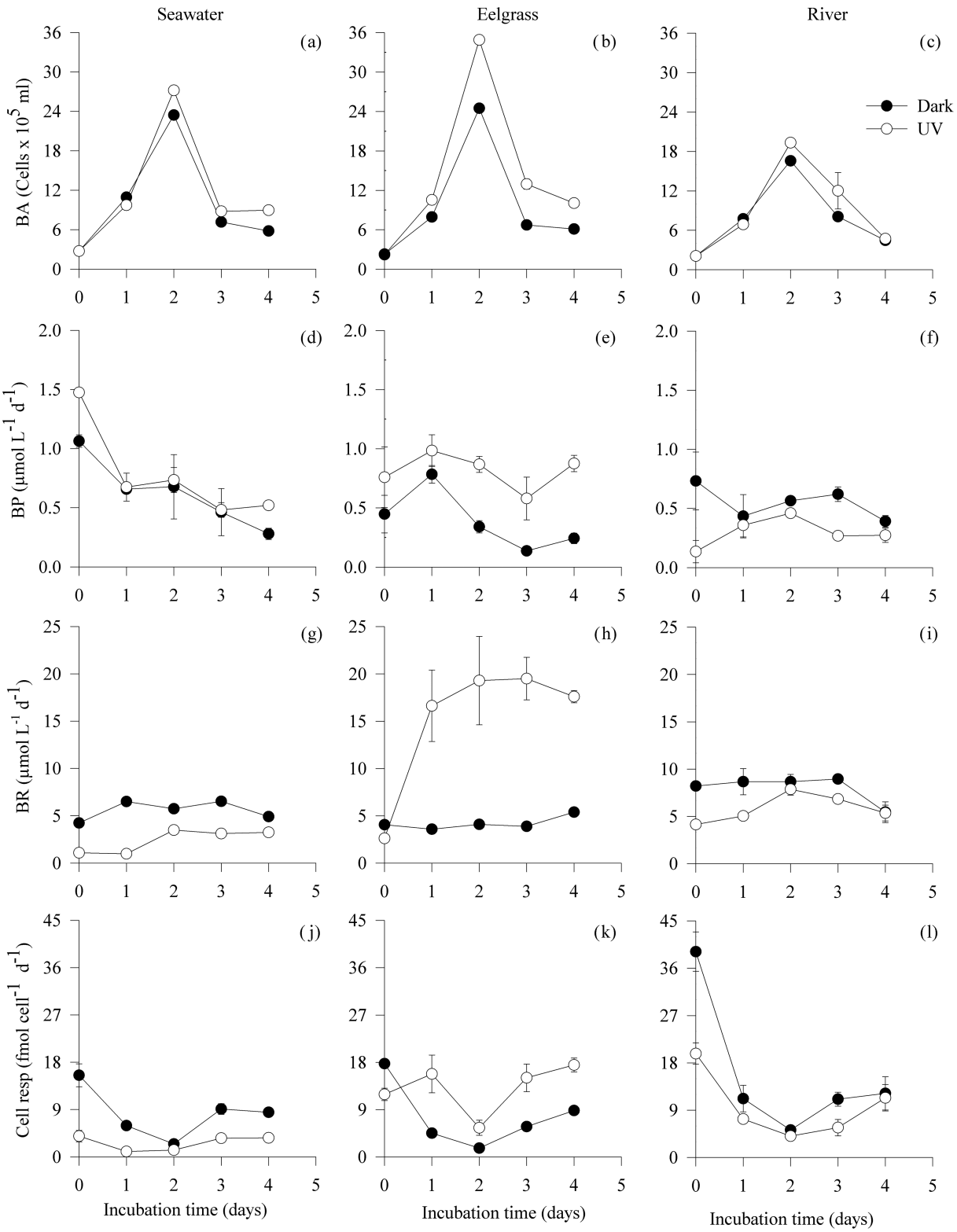


**Figure 3.** Time course changes in bacterial abundance (BA; **a**, **b**, **c**), production (BP; **d**, **e**, **f**), respiration (BR; **g**, **h**, **i**) and cell-specific respiration (Cell resp; **j**, **k**, **l**) during the 4-day incubations in the different experiments (seawater, eelgrass and river). Error bars represent standard deviations; where not visible error bars are within the symbol.

**Table 2.** Initial ($BB_0$, $BP_0$, $BR_0$) and final ($BB_4$, $BP_4$, $BR_4$) bacterial biomass (BB), production (BP), and respiration (BR) are shown together with the bacterial biomass (BG) and specific growth rate at day 0 ($BP_0$/ $BB_0$) and 4 ($BP_4$/ $BB_4$) for the dark and UV exposed samples in the 3 different experiments (seawater, eelgrass and river). Bacterial carbon demand (BCD) and growth efficiency (BGE) at incubation day 0 ($BCD_0$, $BGE_0$) and 4 ($BCD_4$, $BGE_4$), averaged ($BCD_{Avg}$, $BGE_{Avg}$) and integrated values ($BCD_{Int}$, $BGE_{Int}$) for the different experiments are also shown. Values are averages of 3 replicates ± standard error. Bacterial richness (number of distinct OTUs) and bacterial evenness (inverse Simpson index) were estimated from ARISA fingerprinting analyses.

| | Seawater | | Eelgrass | | River | |
|---|---|---|---|---|---|---|
| | Dark | UV | Dark | UV | Dark | UV |
| $BB_0$ ($\mu$mol $L^{-1}$) | 0.27 ± 0.01 | 0.27 ± 0.01 | 0.23 ± 0.01 | 0.22 ± 0.01 | 0.21 ± 0.01 | 0.21 ± 0.02 |
| $BB_4$ ($\mu$mol $L^{-1}$) | 0.58 ± 0.04 | 0.89 ± 0.01 | 0.61 ± 0.02 | 1.00 ± 0.04 | 0.45 ± 0.03 | 0.47 ± 0.03 |
| BG ($\mu$mol $L^{-1}$) | 2.07 ± 0.05 | 2.44 ± 0.03 | 2.22 ± 0.03 | 3.27 ± 0.04 | 1.45 ± 0.04 | 1.72 ± 0.04 |
| $BP_0$ ($\mu$mol $L^{-1}$ $d^{-1}$) | 1.06 ± 0.05 | 1.47 ± 0.02 | 0.45 ± 0.16 | 0.76 ± 0.26 | 0.73 ± 0.24 | 0.14 ± 0.09 |
| $BP_4$ ($\mu$mol $L^{-1}$ $d^{-1}$) | 0.28 ± 0.05 | 0.52 ± 0.02 | 0.24 ± 0.04 | 0.88 ± 0.07 | 0.39 ± 0.05 | 0.27 ± 0.06 |
| $BP_{Int}$ ($\mu$mol $L^{-1}$ $d^{-1}$) | 2.47 ± 0.55 | 2.89 ± 0.31 | 1.61 ± 0.24 | 3.25 ± 0.55 | 2.18 ± 0.42 | 1.29 ± 0.25 |
| $BP_0/BB_0$ ($d^{-1}$) | 3.90 ± 0.01 | 5.41 ± 0.35 | 1.96 ± 0.70 | 3.46 ± 1.26 | 3.50 ± 1.40 | 0.65 ± 0.47 |
| $BP_4/BB_4$ ($d^{-1}$) | 0.48 ± 0.11 | 0.58 ± 0.03 | 0.40 ± 0.09 | 0.87 ± 0.10 | 0.88 ± 0.16 | 0.58 ± 0.17 |
| $BR_0$ ($\mu$mol $L^{-1}$ $d^{-1}$) | 4.23 ± 0.44 | 1.08 ± 0.24 | 4.06 ± 0.15 | 2.61 ± 0.18 | 8.20 ± 0.23 | 4.14 ± 0.33 |
| $BR_4$ ($\mu$mol $L^{-1}$ $d^{-1}$) | 4.90 ± 0.16 | 3.24 ± 0.07 | 5.39 ± 0.18 | 17.59 ± 0.65 | 5.44 ± 1.09 | 5.35 ± 0.83 |
| $BR_{Int}$ ($\mu$mol $L^{-1}$ $d^{-1}$) | 21.18 ± 1.29 | 9.73 ± 0.89 | 14.80 ± 0.76 | 59.52 ± 10.10 | 30.07 ± 3.02 | 22.24 ± 1.65 |
| $BCD_0$ ($\mu$mol $L^{-1}$ $d^{-1}$) | 4.91 ± 0.45 | 2.45 ± 0.24 | 4.13 ± 0.30 | 3.13 ± 0.42 | 8.18 ± 0.46 | 3.90 ± 0.40 |
| $BCD_4$ ($\mu$mol $L^{-1}$ $d^{-1}$) | 4.73 ± 0.20 | 3.46 ± 0.08 | 5.14 ± 0.21 | 16.85 ± 0.66 | 5.34 ± 1.04 | 5.14 ± 0.82 |
| $BCD_{Avg}$ ($\mu$mol $L^{-1}$ $d^{-1}$) | 10.37 ± 2.59 | 28.66 ± 8.87 | 4.21 ± 0.25 | 14.55 ± 2.89 | 7.80 ± 0.62 | 5.61 ± 0.65 |
| $BCD_{Int}$ ($\mu$mol $L^{-1}$ $d^{-1}$) | 23.7 ± 1.7 | 11.7 ± 1.1 | 16.4 ± 1.0 | 62.8 ± 10.6 | 32.3 ± 3.4 | 23.5 ± 1.9 |
| $BGE_0$ (%) | 20 ± 3 | 58 ± 7 | 10 ± 4 | 23 ± 10 | 8 ± 3 | 3 ± 1 |
| $BGE_4$ (%) | 5 ± 1 | 14 ± 1 | 4 ± 1 | 5 ± 1 | 7 ± 2 | 5 ± 2 |
| $BGE_{Avg}$ (%) | 10 ± 3 | 29 ± 9 | 9 ± 3 | 8 ± 4 | 8 ± 3 | 5 ± 1 |
| $BGE_{Int}$ (%) | 11 ± 2 | 25 ± 6 | 11 ± 2 | 6 ± 2 | 5 ± 1 | 7 ± 2 |
| Bacterial richness | 70 | 39 | 66 | 55 | 87 | 54 |

fingerprints (Fig. 5). At the end of the experiments the bacterial community structure significantly differed from the initial community in all dark and UV pre-treated experiments, sharing less than 40% of the Bray–Curtis similarity. A significant effect of DOM origin was observed, with bacterial assemblages from the eelgrass experiments greatly differing from those in the seawater and river experiments (Fig. 5). The UV pre-exposure strongly affected the structure of the bacterial communities in the seawater and river experiments, whereas no significant differences in bacterial community composition were found in the dark and UV treatments in the eelgrass experiment (Fig. 5). Similarly, bacterial richness (number of distinct OTUs) was higher in dark than in the UV treatments in the seawater and river experiments, whereas it was similar in the dark and UV treatments in the eelgrass experiment (Table 2).

## DISCUSSION

The absorption of sunlight by CDOM depends on the intensity of solar radiation, water transparency, and the DOM chemical structure and abundance of functional groups able to absorb light. After absorption by CDOM sunlight initiates photochemically mediated reactions. This can alter the DOM elemental and molecular composition by 1) breaking down large coloured macromolecules into smaller colourless compounds, 2) directly removing DOM by the production of carbon gasses (e.g. CO, $CO_2$) and inorganic nutrients ($HPO_4^{2-}$, $NH_4^+$), and/or 3) enhancing the cross-linking, humification and polymerization of labile biomolecules into more recalcitrant compounds (e.g. Moran and Zepp 1997; Helms *et al.* 2008; Rossel *et al.* 2013; Mopper, Kieber and Stubbins 2015).

In this study, using DOM derived from different natural sources, we found that sunlight exposure impacted the CDOM differently depending on their origin. The largest photodegradation impacts were found on the river- followed by the eelgrass- and seawater-derived DOM, with generally larger impacts on the humic-like compared with the protein-like fluorophores. This suggests that the influence of sunlight varies depending on the initial chemical composition, as also found previously (Moran, Sheldon and Zepp 2000; Stedmon *et al.* 2007; Gonsior *et al.* 2009). In all experiments the FDOM levels were different in the dark and sunlight-exposed samples, while the C-specific CDOM absorption increased in the seawater and eelgrass experiments and decreased in the river experiment (Figs 1 and 2). The increase in the CDOM spectral slope ratio ($S_R$) furthermore demonstrated that the sunlight pre-exposure induced a decrease in the average DOM molecular weight (Helms *et al.* 2008). These differences indicates that the chemical composition and molecular size distribution of the precursor and produced material were different in the river experiment compared with the other experiments (Reitner, Herzig and Herndl 2002; Rossel *et al.* 2013). This is not surprising considering that we only used the high molecular weight fraction (>1 kDa) of the DOM to perform this experiment. The increases in CDOM absorption measured in the seawater and eelgrass experiments (positive values in Fig. 1d) suggests that a 'photohumification' of the DOM pool was taking place, which is linked with the production of new aromatic compounds (Reitner, Herzig and Herndl 2002; Rossel *et al.* 2013). In the past such photohumification processes have been linked with the photochemical degradation of tryptophan (Reitner, Herzig and Herndl 2002; Biers, Zepp and Moran 2007; Bianco *et al.* 2014), and as the CDOM production in the seawater and eelgrass was followed by a decrease in protein-like fluorescence, similar processes to those described in the previous studies could also have taken place in our experiments. In all sunlight-exposed samples the change in CDOM colour was followed by a detectable DOC decrease and a release of $NH_4^+$, with higher production in the CDOM richer incubations (eelgrass and

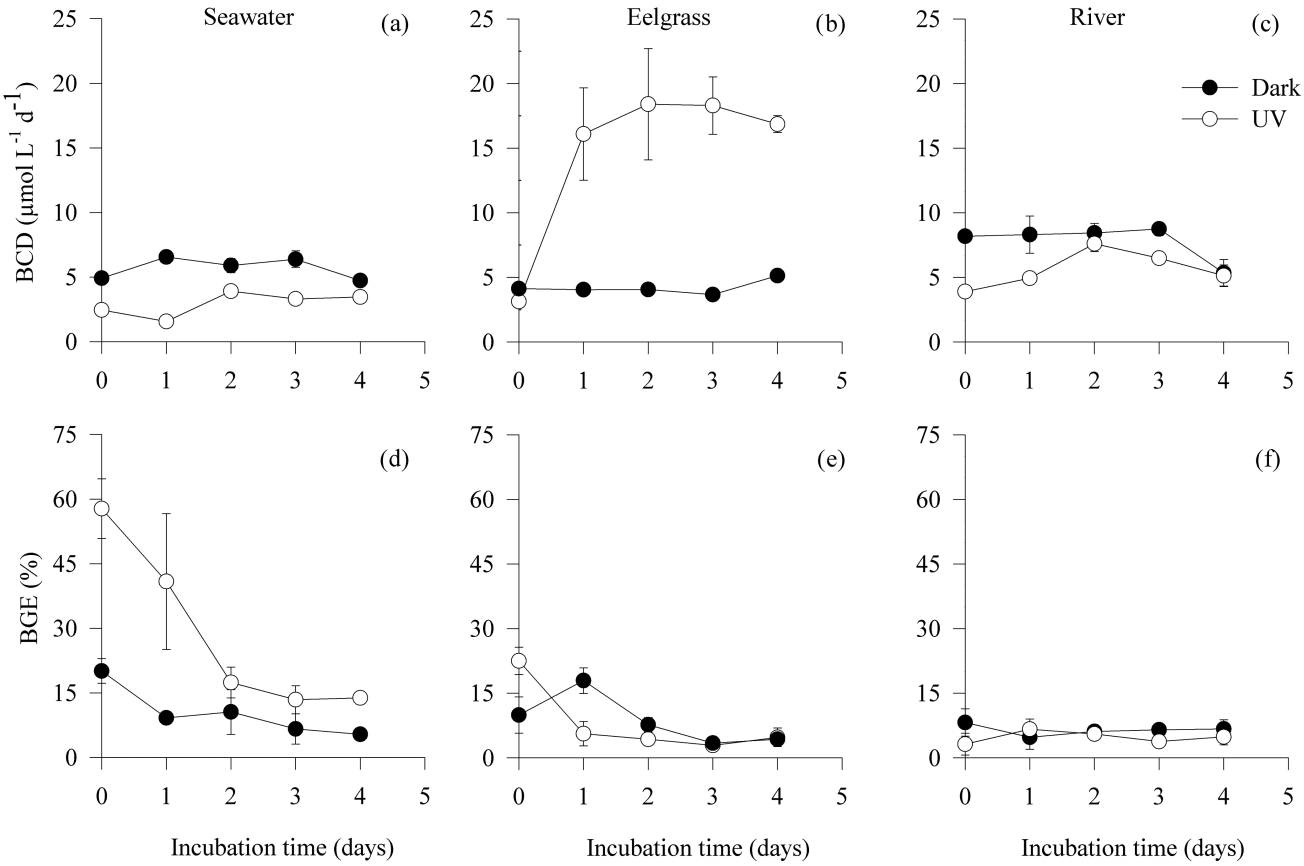


**Figure 4.** Time evolution of bacterial carbon demand (BCD; **a**, **b**, **c**) and growth efficiency (BGE; **d**, **e**, **f**) during the seawater, eelgrass and river experiments. Error bars represent standard deviations.

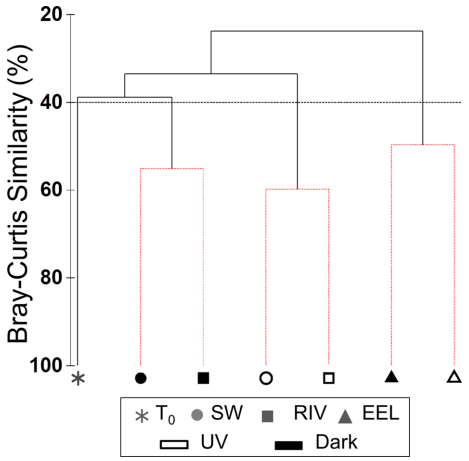


**Figure 5.** Dendrogram plot of the hierarchical cluster analysis (group average mode) based on the bacterial community similarities (Bray–Curtis) between samples at the beginning ($T_0$) and at the end of the seawater (SW), eelgrass (EEL) and river (RIV) experiments. Red dashed branches represent statistically significant clusters ($P < 0.05$) according to the SIMPROF test (999 permutations). Open symbols represent UV treatments and closed symbols represent dark treatments.

river), demonstrating that the coloured compounds are the likely sources of the nutrients produced (Vähätalo and Wetzel 2004; Vähätalo and Järvinen 2007). While the photochemical production of $NH_4^+$ has been demonstrated in numerous studies, the production of $HPO_4^{2-}$, found in the seawater and eelgrass, has not been reported as often; our study therefore suggests that sunlight not only impacts the C and N biogeochemistry, but also potentially P cycling in the Ría de Vigo.

Previous studies have demonstrated both decreases and increases in the DOM bioavailability after sunlight exposure (Mopper, Kieber and Stubbins 2015). Specifically, the increased DOM bioavailability has been linked with the production of new oxygen-rich compounds, and with the degradation of recalcitrant molecules into labile compounds such as amino acids and carbohydrates (Kujawinski *et al.* 2004). On the contrary, the decrease in DOM bioavailability is thought to be connected with the transformation of bioavailable substances into biorecalcitrant compounds and/or the production of reactive oxygen species (ROS), which can inhibit microbial activity (Obernosterer, Reitner and Herndl 1999; Scully, Cooper and Tranvik 2003; Obernosterer and Benner 2004). The variable results in previous studies have been linked with changes in the predominant source of DOM, with some studies suggesting that systems dominated by terrestrial material (allochthonous) will experience an increased microbial activity with sunlight exposure, while decreases should be found in plankton-dominated (autochthonous) systems (Kieber, Daniel and Mopper 1989; Moran and Zepp 1997; Benner and Biddanda 1998; Obernosterer, Reitner and Herndl 1999). Our results suggest that bacterial degradation of DOC from different sources is differently impacted by solar radiation. The seawater and river experiments showed lower bioavailable DOC, microbial activity and carbon demand upon UV exposure, as was also previously found for seawater collected during autumn and winter in the Ría de Vigo (Lønborg *et al.* 2013).

Contrarily, the eelgrass experiment showed enhanced bioavailable DOC levels, microbial activity and carbon demand (Figs 3 and 4, and Table 2). These responses could be linked with the difference in chemical composition of the initial and photoproduced DOM, as indicated by the different response in FDOM signals and production of inorganic nutrients ($HPO_4^{2-}$ and $NH_4^+$) in the sunlight-exposed samples. The response could also be connected with a difference in the conversion of bioavailable substrates to DIC and other C gases, production of substances inhibiting microbes (e.g. ROS), release of toxic metals (e.g. Cd and Hg) from DOM complexes and the photochemical production of more recalcitrant compounds (Mopper, Kieber and Stubbins 2015). Humic substances and amino acids (e.g. tryptophan) are known to absorb and undergo photochemical degradation, which can provide a new source of ROS (Creed 1984; Anesio *et al.* 2005; Biers, Zepp and Moran 2007; Mayer *et al.* 2009). While some ROS species (mainly OH radicals) can stimulate microbial activity by the production of labile substrates, others have been shown to destroy biologically labile compounds and/or cause oxidative stress (Scully, Cooper and Tranvik 2003; Pullin *et al.* 2004; Lesser 2006; Tedetti *et al.* 2009). In our study we found a reduction in the humic and protein-like fluorescence signals and a decreased BCD on the initial day in the sunlight pre-exposed samples, suggesting that a short lived inhibitor such as ROS was influencing our results. The sunlight induced changes in DOM bioavailability deserves more attention as this could represent a source of recalcitrant material that accumulates in the ocean over longer time scales, and as such these processes could be an important abiotic equivalent to the microbial carbon pump (Jiao *et al.* 2010). As these photochemically mediated processes could represent an important source of recalcitrant material and our study was not designed to study these processes in detail, we suggest that future studies use a more detailed approach towards understanding the impact of these processes.

The bacterial growth efficiency (BGE), which describes the relation between respiration and biomass production, has previously been reported to be unaffected, increased and decreased upon DOC sunlight exposure (e.g. Pullin *et al.* 2004; Smith and Benner 2005; Abboudi *et al.* 2008; Lønborg *et al.* 2013). The initial and integrated BGE varied in this study between $3 \pm 1$ and $58 \pm 7\%$, which is comparable to values previously reported for the Ría de Vigo (range 7–55%: Lønborg *et al.* 2011) and values found for marine systems in general (average 20%: del Giorgio and Cole 1998). The initial BGE was on average higher in the sunlight-exposed seawater and eelgrass samples while lower values were found in the river experiments (Table 2). In all experiments, changes in the instantaneous and integrated BGE were mainly driven by respiration relative to production, as also found in previous studies (Pullin *et al.* 2004; Smith and Benner 2005; Amado *et al.* 2006). The lower integrated BGE found in the dark seawater and UV eelgrass samples suggest that the bacterial community in these incubations used more energy to produce the same biomass and that BP and BR responded differently to photo-altered DOM. In coastal waters where the importance of different DOM sources varies spatially and with season (Cauwet 2002), and the DOM chemical composition might change in the future due to factors such as increased loads from the catchment (Lennon *et al.* 2013) and changes in upwelling intensity (Gago *et al.* 2011). Our results demonstrate that the bacterial transfer of energy and nutrients to the microbial food web will change depending on the DOM composition and whether these compounds are exposed to sunlight. The microbial community may react to differences in the substrate supply and composition by physiological acclimation and/or might force a shift in the community structures (Abboudi *et al.* 2008; Piccini *et al.* 2009; Lønborg *et al.* 2013). Here, we used ARISA as a genetic fingerprint to characterize the changes in bacterial diversity during our incubations. This technique uses the length heterogeneity of the PCR amplified highly variable intergenic spacer region between the 16S and 23S rRNA genes. This does not allow a complete characterization of the microbial community but lets us detect both dominant and moderately abundant marine planktonic bacteria taxa (Dorst *et al.* 2014), allowing us to analyse bacterial diversity patterns with relatively high resolution. In our experiments we found differences in the DOC utilization, bacterial production, respiration and growth efficiencies between the DOM sources and treatments (dark and UV). This also resulted in bacterial richness and community composition changes associated with photoalteration of DOM in the seawater and river experiments but not for the eelgrass experiment. This indicates that the dark and UV exposure plays an important role in distinguishing the communities developed using DOM that are prevalent in the Ría de Vigo (from seawater and river sources). Nevertheless the effect of the UV radiation is secondary when the available DOM in the experiment (eelgrass extracts) is scarce; in this case microbial diversity is driven by the DOM origin. This contrasts with the important changes in metabolic rates after eelgrass-derived DOM had been exposed to sunlight.

Previous studies have demonstrated shifts in the community structure in response to varying DOM source and photodegradation patterns, which might reflect different strategies and physiological differences in growth rates and enzyme activities (Abboudi *et al.* 2008; Calza *et al.* 2008; Piccini *et al.* 2009; Lønborg *et al.* 2013). This may suggest that, in the eelgrass DOM experiment, UV exposure promotes quantitative rather than qualitative changes in DOM and nutrient pools. By contrast photoalteration of seawater- and river-derived DOM appears to promote similar changes in bacterial community composition, which suggest that UV exposure promotes important qualitative changes in DOM composition or inorganic nutrient pools that largely influence bacterial diversity. Surprisingly, the bacterial community developed in the dark treatments did not significantly differ between seawater and river experiments, despite the important quantitative and qualitative differences of the DOM pool. This indicates that the concentration of inorganic nutrients, which significantly increased after UV exposure of seawater and river DOM, could be a major driver of the bacterial community composition.

In conclusion, we suggest that (i) the bacterial transfer of energy and nutrients to the microbial food web in the Ría de Vigo depends on the predominant DOM source, showing that changes in the microbial response to photo-altered DOM is likely linked to differences in initial chemical composition; and (ii) the concentration of inorganic nutrients, which significantly increased after UV exposure of seawater and river DOM, could be a major driver of the bacterial community composition.

## ACKNOWLEDGEMENTS

This study was partly funded by the Swansea University Research Fund, a EUROMARINE Fellowship and the Australian Institute of Marine Science. We also would like to thank J. Herrera Cortijo and J. Fernandez for their help collecting the seawater and to V. Vieitez and M. J. Pazó for their very skilful analysis of the fluorescence, inorganic nutrient and DOM samples. M.N.-C. was supported by the CSIC Program 'Junta para la Ampliación de Estudios' co-financed by the ESF. We also thank the two anonymous reviewers for valuable comments on the manuscript.

***Conflict of interest.*** None declared.

## REFERENCES


Abboudi M, Jeffrey WH, Ghiglione J-F *et al*. Effects of photochemical transformations of dissolved organic matter on bacterial metabolism and diversity in three contrasting coastal sites in the northwestern Mediterranean sea during summer. *Microb Ecol* 2008;**55**:344–57.

Anesio AM, Graneli W, Aiken GR *et al*. Effect of humic substance photodegradation on bacterial growth and respiration in lake water. *Appl Environ Microbiol* 2005;**71**:6267–75.

Amado AM, Farjalla VF, Esteves de AF *et al*. Complementary pathways of dissolved organic carbon removal pathways in clear-water Amazonian ecosystems: photochemical degradation and bacterial uptake. *FEMS Microbiol Ecol* 2006;**56**:8–17.

Apple JK, del Giorgio PA. Organic substrate quality as the link between bacterioplankton carbon demand and growth efficiency in a temperate salt-marsh estuary. *ISME J* 2007;**1**: 729–42.

Benner R, Biddanda B. Photochemical transformations of surface and deep marine dissolved organic matter: effects on bacterial growth. *Limnol Ocean* 1998;**43**:1373–8.

Benner R, Ziegler S. Do photochemical transformations of dissolved organic matter produce biorefractory as well as bioreactive substrates? In: Bell CR, Brylinsky M, Johnson-Green PC (eds). *Microbial Biosystems: New Frontiers. Proceedings of the 8th International Symposium on Microbial Ecology, 1998*. Halifax: Atlantic Canada Society for Microbial Ecology, 2000, 181–92.

Bianco A, Minella M, De Laurentiis E *et al*. Photochemical generation of photoactive compounds with fulvic-like and humic-like fluorescence in aqueous solution. *Chemosphere* 2014;**111**:529–36.

Biers EJ, Zepp RG, Moran MA. The role of nitrogen in chromophoric and fluorescent dissolved organic matter formation. *Mar Chem* 2007;**103**:46–60.

Calza P, Massolino C, Pelizzetti E *et al*. Solar driven production of toxic halogenated and nitroaromatic compounds in natural seawater. *Sci Total Environ* 2008;**398**:196–202.

Cardinale M, Brusetti L, Quatrini P *et al*. Comparison of different primer sets for use in automated ribosomal intergenic spacer analysis of complex bacterial communities. *Appl Environ Microbiol* 2004;**70**:6147–56.

Cauwet G. DOM in coastal areas. In: Hansell DA, Carlson CA (eds). *Biogeochemistry of Marine Dissolved Organic Matter*. San Diego: Academic Press, 2002, 579–609.

Cooper WJ, Zika RG, Petasne RG *et al*. Sunlight-induced photochemistry of humic substances in natural waters: major reactive species. In: Suffet IH, MacCarthy P (eds). *Aquatic Humic Substances: Influence on Fate and Treatment of Pollutants*. Washington: American Chemical Society, 1989, 333–62.

Coble PG. Characterization of marine and terrestrial DOM in seawater using excitation–emission matrix spectroscopy. *Mar Chem* 1996;**51**: 325–46.

Creed D. The photophysics and photochemistry of near-UV absorbing amino acids – I. Tryptophan and its simple derivatives. *Photochem Photobiol* 1984;**39**:531–62.

Del Giorgio PA, Cole JJ. Bacterial growth efficiency in natural aquatic systems. *Annu Rev Ecol Syst* 1998;**29**:503–41.

Dorst J, Bissett A, Palmer AS *et al*. Community fingerprinting in a sequencing world. *FEMS Microbiol Ecol* 2014;**89**:316–30.

Fuhrman JA, Azam F. Bacterioplankton secondary production estimates for coastal waters of British Columbia, Antarctica, and California. *Appl Environ Microbiol* 1980;**36**:1085–95.

Fuhrman JA, Hewson I, Schwalbach M *et al*. Annually reoccurring bacterial communities are predictable from ocean conditions. *Proc Natl Acad Sci U S A* 2006;**103**:13104–9.

Fukuda R, Ogawa H, Nagata T *et al*. Direct determination of carbon and nitrogen contents of natural bacterial assemblages in marine environments. *Appl Environ Microbiol* 1998;**64**: 3352–8.

Gago J, Álvarez-Salgado XA, Nieto-Cid M *et al*. Continental inputs of C, N, P and Si species to the Ría de Vigo (NW Spain). *Estuar Coast Shelf Sci* 2005;**65**:74–82.

Gago J, Cabanas JM, Casas G *et al*. Thermohaline measurements in the continental shelf zone of the NW Iberian Peninsula. *Clim Res* 2011;**48**:219–29.

Giovannoni SJ, Vergin KL. Seasonality in ocean microbial communities. *Science* 2012;**335**:671–6.

Gonsior M, Peake BM, Cooper WT *et al*. Photochemically induced changes in dissolved organic matter identified by ultrahigh resolution Fourier transform ion cyclotron resonance mass spectrometry. *Environ Sci Technol* 2009;**43**:698–703.

Hansen HP, Koroleff F. Automated chemical analysis. In: Grasshoff K, Kermling K, Ehrhardt M (eds). *Methods of Seawater Analysis*. Weinheim: Wiley-VCH, 1999, 159–226.

Hedges JI. Why dissolved organic matter? In: Hansell DA, Carlson CA (eds). *Biogeochemistry of Marine Dissolved Organic Matter*. San Diego: Academic Press, 2002, 1–33.

Helms JR, Stubbins A, Ritchie JD *et al*. Absorption spectral slopes and slope ratios as indicators of molecular weight, source, and photobleaching of chromophoric dissolved organic matter. *Limnol Oceanogr* 2008;**53**:955–69.

Jiao N, Herndl GJ, Hansell DA *et al*. Microbial production of recalcitrant dissolved organic matter: long-term carbon storage in the global ocean. *Nat Rev Microbiol* 2010;**8**:593–9.

Kawasaki N, Benner R. Bacterial release of dissolved organic matter during cell growth and decline: Molecular origin and composition. *Limnol Oceanogr* 2006;**51**:2170–80.

Kieber DJ, Daniel JM, Mopper K. Photochemical source of biological substrates in sea water: implications for carbon cycling. *Nature* 1989;**341**:637–39.

Kieber RJ, Hydro LH, Seaton PJ. Photooxidation of triglycerides and fatty acids in seawater: implication toward the formation of marine humic substances. *Limnol Oceanogr* 1997;**42**:1454–62.

Kujawinski EB, Del Vecchio R, Blough NV *et al*. Probing molecular-level transformations of dissolved organic matter: insights on photochemical degradation and protozoan modification of DOM from electrospray ionization Fourier transform ion cyclotron resonance mass spectrometry. *Mar Chem* 2004;**92**:23–37.

Lawaetz AJ, Stedmon CA Fluorescence intensity calibration using raman scatter peak of water. *Appl Spectrosc* 2009;**63**: 936–40.

Lennon JT, Hamilton SK, Muscarella ME *et al*. A source of terrestrial organic carbon to investigate the browning of aquatic ecosystems. *PLoS One* 2013;**8**:e75771.

Lesser MP. Oxidative stress in marine environments: Biochemistry and physiological ecology. *Annu Rev Physiol* 2006;**68**: 253–78.

Lønborg C, Álvarez-Salgado XA. Recycling versus export of bioavailable dissolved organic matter in the coastal ocean and efficiency of the continental shelf pump. *Global Biogeochem Cycl* 2012;**26**, DOI: 10.1029/2012GB004353.

Lønborg C, Álvarez-Salgado XA, Davidson K *et al*. Production of bioavailable and refractory dissolved organic matter by coastal heterotrophic microbial populations. *Estuar Coast Shelf Sci* 2009;**82**:682–8.

Lønborg C, Álvarez-Salgado XA, Davidson K *et al*. Assessing the microbial bioavailability and degradation rate constants of

dissolved organic matter by fluorescence spectroscopy in the coastal upwelling system of the Ría de Vigo. *Mar Chem* 2010b;**119**:121–9.

Lønborg C, Álvarez-Salgado XA, Martínez-García SE *et al.* Stoichiometry of dissolved organic matter and the kinetics of its microbial degradation in a coastal upwelling system. *Aquat Microb Ecol* 2010a;**58**:117–26.

Lønborg C, Álvarez-Salgado XA, Martínez-Garcia S *et al.* Carbon cycling and bacterial growth efficiency in a coastal upwelling system (NW Iberian Peninsula). *Aquat Microb Ecol* 2011;**63**:183–91.

Lønborg C, Martínez-Garcia S, Teira E *et al.* Effects of the photochemical transformation of dissolved organic matter on bacterial physiology and diversity in a coastal system. *Estuar Coast Shelf Sci* 2013;**129**:11–8.

Martínez-García SE, Fernández E, Aranguren-Gassis M *et al.* In vivo electron transport system activity: a method to estimate respiration in natural marine microbial planktonic communities. *Limnol Oceanogr Methods* 2009;**7**:459–69.

Mayer LM, Schick LL, Bianchi TS *et al.* Photochemical changes in chemical markers of sedimentary organic matter source and age. *Mar Chem* 2009;**113**:123–8.

Miller WL, Moran MA. Interaction of photochemical and microbial processes in the degradation of refractory dissolved organic matter from a coastal marine environment. *Limnol Oceanogr* 1997;**42**: 1317–24.

Miller WL, Zepp RG. Photochemical production of dissolved inorganic carbon from terrestrial organic matter: significance to the oceanic organic carbon cycle. *Geophys Res Lett* 1995;**22**:417–20.

Mopper K, Kieber D, Stubbins A. Marine photochemistry of organic matter: processes and impacts. In: Hansell DA, Carlson CA (eds). *Biogeochemistry of Marine Dissolved Organic Matter*, 2nd edn. Burlington: Academic Press, 2015, 389–50.

Moran MA, Sheldon WM, Zepp RG. Carbon loss and optical property changes during long-term photochemical and biological degradation of estuarine dissolved organic matter. *Limnol Oceanogr* 2000;**45**:1254–64.

Moran MA, Zepp RG. Role of photoreactions in the formation of biologically labile compounds from dissolved organic matter. *Limnol Oceanogr* 1997;**42**:1307–16.

Nogueira E, Pérez FF, Ríos AF. Seasonal patterns and long-term trends in an estuarine upwelling ecosystem (Ría de Vigo, NW Spain). *Estuar Coast Shelf Sci* 1997;**44**:285–300.

Obernosterer I, Benner R. Competition between biological and photochemical processes in the mineralization of dissolved organic carbon. *Limnol Oceanogr* 2004;**49**:117–24.

Obernosterer I, Reitner B, Herndl GJ. Contrasting effects of solar radiation on dissolved organic matter and its bioavailability to marine bacterioplankton. *Limnol Oceanogr* 1999;**44**: 1645–54.

Piccini C, Conde D, Pernthaler J *et al.* Alteration of chromophoric dissolved organic matter by solar UV radiation causes rapid changes in bacterial community composition. *Photochem Photobiol Sci* 2009;**8**:1321–8.

Pullin MJ, Bertilsson S, Goldstone JV *et al.* Effects of sunlight and hydroxyl radical on dissolved organic matter: bacterial growth efficiency and production of carboxylic acids and other substrates. *Limnol Oceanogr* 2004;**49**:2011–22.

Ramette A. Quantitative community fingerprinting methods for estimating the abundance of operational taxonomic units in natural microbial communities. *Appl Environ Microbiol* 2009;**75**:2495–505.

Reitner B, Herzig A, Herndl GJ. Photoreactivity and bacterioplankton availability of aliphatic versus aromatic amino acids and a protein. *Aquat Microb Ecol* 2002;**26**:305–11.

Reinthaler T, Winter C, Herndl GJ. Relationship between bacterioplankton richness, respiration, and production in the Southern North Sea. *Appl Environ Microbiol* 2005;**71**:2260–6.

Rivkin RB, Anderson MR. Inorganic nutrient limitation of oceanic bacterioplankton. *Limnol Oceanogr* 1997;**42**:730–40.

Rivkin RB, Legendre L. Biogenic carbon cycling in the upper ocean: Effects of microbial respiration. *Science* 2001;**291**: 2398–400.

Rossel PE, Vähätalo AV, Witt M *et al.* Molecular composition of dissolved organic matter from a wetland plant (*Juncus effusus*) after photochemical and microbial decomposition (1.25 yr): Common features with deep sea dissolved organic matter. *Org Geochem* 2013;**60**:62–71.

Scully NM, Cooper WJ, Tranvik LJ. Photochemical effects on microbial activity in natural waters: the interaction of reactive oxygen species and dissolved organic matter. *FEMS Microb Ecol* 2003;**46**:353–7.

Smith EM, Benner R. Photochemical transformations of riverine dissolved organic matter: effects on estuarine bacterial metabolism and nutrient demand. *Aquat Microb Ecol* 2005;**40**:37–50.

Sobczak WV, Cloern JE, Jassby AD *et al.* Detritus fuels ecosystem metabolism but not metazoan food webs in San Francisco estuary freshwater delta. *Estuaries* 2005;**28**:124–37.

Sokal FF, Rohlf FJ. *Biometry*. New York: Freeman, 1995.

Søndergaard M. Kinetics of extracellular release of $^{14}$C-labelled organic carbon by submerged macrophytes. *Oikos* 1981;**36**:331–47.

Stedmon CA, Markager S, Tranvik L *et al.* Photochemical production of ammonium and transformation of dissolved organic matter in the Baltic Sea. *Mar Chem* 2007;**104**:227–40.

Sulzberger B, Durisch-Kaiser E. Chemical characterization of dissolved organic matter (DOM): a prerequisite for understanding UV-induced changes of DOM absorption properties and bioavailability. *Aquat Sci* 2009;**71**:104–26.

Tedetti M, Joux F, Charrière B *et al.* Contrasting effects of solar radiation and nitrates on the bioavailability of dissolved organic matter to marine bacteria. *Photochem Photobiol A Chem* 2009;**201**:243–7.

Tranvik LJ, Bertilsson S. Contrasting effects of solar UV radiation on dissolved organic sources for bacterial growth. *Ecol Lett* 2001;**4**:458–63.

Vähätalo AV, Järvinen M. Photochemically produced bioavailable nitrogen from biologically recalcitrant dissolved organic matter stimulates production of a nitrogen-limited microbial food web in the Baltic Sea. *Limnol Oceanogr* 2007;**52**: 132–43.

Vähätalo AV, Wetzel RG. Photochemical and microbial decomposition of chromophoric dissolved organic matter during long (months – years) exposures. *Mar Chem* 2004; **89**:313–26.

Weishaar JL, Aiken GR, Bergamaschi BA *et al.* Evaluation of specific ultraviolet absorbance as an indicator of the chemical composition and reactivity of dissolved organic carbon. *Environ Sci Technol* 2003;**37**:4702–8.

Wollast R. Evaluation and comparison of the global carbon cycle in the coastal zone and in the open ocean. In: Brink KH, Robinson AR (eds). *The Sea, the Global Coastal Ocean, Processes and Methods*. Hoboken: John Wiley, 1998, 213–52.